Enhanced Ferromagnetism and Tunable Saturation Magnetization of Mn/C-Codoped GaN Nanostructures Synthesized by Carbothermal Nitridation

ARTICLE *in* JOURNAL OF THE AMERICAN CHEMICAL SOCIETY · NOVEMBER 2008

Impact Factor: 12.11 · DOI: 10.1021/ja807030v · Source: PubMed

J|A|C|S
ARTICLES

Published on Web 11/12/2008

Enhanced Ferromagnetism and Tunable Saturation Magnetization of Mn/C-Codoped GaN Nanostructures Synthesized by Carbothermal Nitridation

Zeyan Wang,[†] Baibiao Huang,*[,†] Lin Yu,[‡] Ying Dai,[‡] Peng Wang,[†] Xiaoyan Qin,[†] Xiaoyang Zhang,[†] Jiyong Wei,[†] Jie Zhan,[†] Xiangyang Jing,[†] Haixia Liu,[†] and Myung-Hwan Whangbo[§]

State Key Laboratory of Crystal Materials and School of Physics, Shandong University, Jinan 250100, People's Republic of China, and Department of Chemistry, North Carolina State University, Raleigh, North Carolina 27695-8204

Received September 10, 2008; E-mail: bbhuang@sdu.edu.cn

Abstract: Mn/C-codoped GaN nanostructures were synthesized by carbothermal nitridation with active charcoal as the carbon source. Nanostructures such as zigzag nanowires and nanoscrews were observed by varying the reaction time and the C/Ga molar ratio of the starting material used for the synthesis. The structures and morphologies of the as-grown samples were characterized by X-ray diffraction, scanning electron microscopy, and high-resolution transmission electron microscopy measurements. The doping of both Mn and C in the GaN matrix was confirmed by X-ray photoelectron spectroscopy measurements, and the ferromagnetic properties of Mn/C-codoped GaN samples were confirmed by room-temperature magnetization measurements. The saturation magnetization of Mn/C-codoped GaN increases steadily with increasing C/Ga molar ratio of the starting material at a rate of ~0.023 emu/g per C/Ga molar ratio, and the ferromagnetism of Mn/C-codoped GaN can be stronger than that of Mn-doped GaN by a factor of ~40. A plausible growth mechanism was proposed, and the role of carbon codoping in tuning the morphology and ferromagnetic property was discussed. Our work suggests that carbon doping in the GaN matrix favors the N sites over the Ga sites, Mn/C-codoping in the GaN matrix is energetically favorable, and the C-codoping strongly enhances the preference of the FM coupling to the AFM coupling between the two doped Mn sites. These suggestions were probed on the basis of first-principles density functional theory electronic structure calculations for a number of model doped structures constructed with a 32-atom $2 \times 2 \times 2$ supercell.

1. Introduction

The direct-band-gap semiconductor gallium nitride (GaN) is an attractive material for important applications such as blue optoelectronics, high-power and high-frequency devices, and photocatalysts.[1−3] After the discovery of ferromagnetism with a high Curie temperature in Mn-doped GaN,[4,5] there has been intense interest in the fabrication of GaN-based diluted magnetic semiconductors with the primary goal of realizing a room-temperature ferromagnet, a potential candidate for future spintronics applications.[6,7] A number of approaches have been explored to synthesize single-phase Mn-doped GaN, which include epitaxial growth, chemical vapor deposition (CVD), pulse laser deposition, and sputtering.[8−11] The direct nitridation of a mixture of Ga_2O_3 and MnO_2 powders by ammonia, NH_3, is a simple way of preparing Mn-doped GaN[12] and is economical for large-scale production. However, an incomplete nitridation of the intermediate gallium oxynitride (GaO_xN_y) can introduce oxygen contamination into Mn-doped GaN to form donor states,[13] thereby affecting its ferromagnetism.[7] Carbothermal reduction has been demonstrated to be an effective way of reducing residual oxygen atoms in Mn-doped GaN.[14] However, it has not been systemically investigated how the morphology and ferromagnetism of Mn-doped GaN depend on

[†] State Key Laboratory of Crystal Materials, Shandong University.
[‡] School of Physics, Shandong University.
[§] North Carolina State University.

(1) Kim, H.-M.; Cho, Y.-H.; Lee, H.; Kim, L. I.; Ryu, S. R.; Kim, D. Y.; Kang, T. W.; Chung, K. S. *Nano Lett.* **2004**, *4*, 1059.
(2) Liu, B.; Bando, Y.; Tang, C.; Xu, F.; Hu, J.; Golberg, D. *J. Phys. Chem. B* **2005**, *109*, 17082.
(3) Fujii, K.; Ohkawa, K. *J. Electrochem. Soc.* **2006**, *153*, A468.
(4) Dietl, T.; Ohno, H.; Matsukura, F. *Science* **2000**, *287*, 1019.
(5) Reed, M. L.; El-Masry, N. A.; Stadelmaier, H. H.; Ritums, M. K.; Reed, M. J.; Parker, C. A.; Roberts, J. C.; Bedair, S. M. *Appl. Phys. Lett.* **2001**, *79*, 3473.
(6) Wolf, S. A.; Awschalom, D. D.; Buhrman, R. A.; Daughton, J. M.; von Molnar, S.; Roukes, M. L.; Chtchelkanova, A. Y.; Treger, D. M. *Science* **2001**, *294*, 1488.
(7) For a review, see: (a) Liu, C.; Yun, F.; Morkoç, H. *J. Mater. Sci.: Mater. Electron.* **2005**, *16*, 555.
(8) Radovanovic, P. V.; Barrelet, C. J.; Gradecak, S.; Qian, F.; Lieber, C. M. *Nano Lett.* **2005**, *5*, 1407.
(9) Xu, C.; Chun, J.; Lee, H. J.; Jeong, Y. H.; Han, S. E.; Kim, J. J.; Kim, D. E. *J. Phys. Chem. C* **2007**, *111*, 1180.
(10) Ham, M.-H.; Oh, D.-K.; Myoung, J.-M. *J. Phys. Chem. C* **2007**, *111*, 11480.
(11) Leite, D. M. G.; da Silva, L. F.; Pereira, A. L. J.; Dias da Silva, J. H. *J. Cryst. Growth* **2006**, *294*, 309.
(12) Lorenz, M. R.; Binkowshi, B. *J. Electrochem. Soc.* **1962**, *109*, 24.
(13) Jung, W. S. *Mater. Lett.* **2004**, *60*, 2954.
(14) Janik, J. F.; Drygaś, M.; Czosnek, C.; Kamińska, M.; Palczewska, M.; Paine, R. T. *J. Phys. Chem. Solids* **2004**, *65*, 639.

10.1021/ja807030v CCC: $40.75

the C/Ga molar ratio of the starting material used for the synthesis.

In this work, we synthesized Mn/C-codoped GaN by carbothermal nitridation and characterized the as-grown samples by various physical property measurements and first-principles density functional theory (DFT) electronic structure calculations. In our synthesis, activated charcoal was used as the carbon source, and the C/Ga molar ratio in the starting material was systematically varied. Our work shows that the saturation magnetization of Mn/C-codoped GaN can be made greater than that of Mn-doped GaN by a factor of ~40 and that the saturation magnetization of as-grown samples can be tuned by changing the C/Ga molar ratio in the starting mixture. First-principles DFT calculations were carried out for a number of model doped structures constructed with a 32-atom $2 \times 2 \times 2$ supercell to confirm the suggestions of our experimental work that carbon doping in GaN favors the N sites over the Ga sites and that Mn/C-codoping in the GaN matrix is energetically favorable.

2. Experimental Section

Mn/C-codoped GaN samples were prepared by carbothermal nitridation using Ga_2O_3 (99.99%) and MnO_2 (99.9%) as the starting material with activated charcoal as the carbon source. The amount of MnO_2 was set to 5 atom % considering the solubility limit of Mn in GaN. In our synthesis, six different compositions of the starting material (i.e., C/Ga molar ratios of 1/10, 1/5, 1/2, 1/1, and 5/1) were examined. The starting chemicals were mixed and ground uniformly, and the mixture was transferred to a quartz boat located at the center of a quartz tube, which was horizontally placed in a tubular furnace. Then the mixture was heated to 1123 K at a rate of 25 K/min under a flow of NH_3 at 300 sccm and was kept at 1123 K for 180 min. At the end of the heating period, the quartz tube was cooled to room temperature naturally. The ammonia flow was continued until the quartz tube had reached 573 K.

The structures and the morphologies of the as-grown samples were characterized using scanning electron microscopy (SEM) (Hitachi S-4800), X-ray powder diffraction (XRD) (Bruker AXS D8 advance powder diffractometer with a Cu Kα X-ray tube), high-resolution transmission electron microscopy (HR-TEM) (JEOL JEM-2100, 200 kV), and X-ray photoelectron spectroscopy (XPS) (VG MicroTech ESCA 3000 X-ray photoelectron spectroscope using monochromatic Al Kα with a photon energy of 1486.6 eV at a pressure of $>1 \times 10^{-9}$ Torr, a pass energy of 40 eV, an electron takeoff angle of 60°, and an overall resolution of 0.05 eV). The XPS spectra were fitted using a combined polynomial and Shirley-type background function. The magnetic properties of the as-grown samples were examined at room temperature using an alternating gradient magnetometer, MICROMAG 2900 (Princeton Measurement Corp.).

3. Morphology and Crystal Structure

Figure 1 compares the XRD patterns of the as-grown samples GaN and MnO. The major diffraction peaks of all samples correspond to those of the hexagonal wurtzite GaN phase. The XRD peaks marked with asterisks arise from cubic MnO. With increasing C/Ga molar ratio, the XRD peak belonging to MnO decreases in height and completely disappears for the as-grown sample obtained from the highest C/Ga molar ratio (i.e., 5/1). Janik et al.[14] reported that the use of methanol as the carbon source has no impact on the amount of MnO produced, due probably to the low amount of carbon pyrolyzed from methanol in their experiment.

The average sizes of the crystallites of the as-grown samples were estimated on the basis of the Scherrer formula

$$d = \frac{k\lambda}{B \cos \theta}$$

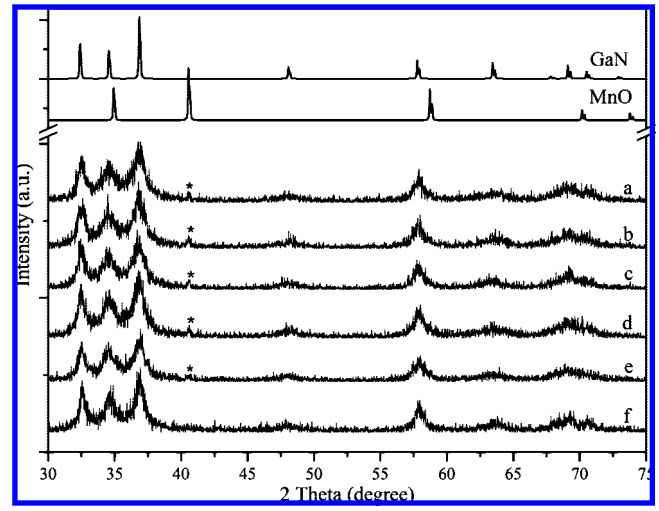

Figure 1. XRD patterns for the as-grown samples of Mn-doped GaN from the starting mixture with C/Ga molar ratios of (a) 1/10, (b) 1/5, (c) 1/2, (d) 1/1, (e) 2/1, and (f) 5/1. For comparison, the XRD patterns of GaN and MnO are also shown. The peaks marked with asterisks show the MnO phase formed during the nitridation process.

where d is the average diameter of the crystallites of the powder sample, k is a constant (usually 0.9), λ is the wavelength of the Cu Kα radiation (i.e., 1.54056 Å), B is the full width at half-maximum of the diffraction peak, and θ is the Bragg angle. The average crystallite sizes of the as-grown samples are calculated to be 8.1, 8.6, 9.6, 11.1, 12.9, and 14.7 nm for samples a, b, c, d, e, and f, respectively.

The morphologies of the as-grown samples were characterized by SEM. As shown in Figure 2a,b, the samples obtained from the starting mixture with a low C/Ga ratio show a porous clodlike structure of 10−20 nm agglomerated from many small nanoparticles with sizes of 10−30 nm. As mentioned above, the crystallite size calculated from the Scherrer formula, ranging from 8 to 15 nm, is the average size of crystal grains. However, the SEM images show nanostructures with sizes of 50−100 nm. Most likely, the latter are made up of many small crystal grains. When the C/Ga molar ratio increases to 1/2, nanowires begin to appear at the edge of the porous clodlike structure (Figure 2c). The nanowires of Mn-doped GaN synthesized by the CVD method exhibit a smooth surface and constant radius,[9] but those obtained in our synthesis have a zigzag structure with a rough surface. They are typically several micrometers long with a thickness of about several tens to 100 nm. For the as-grown samples obtained from the higher C/Ga molar ratio (i.e., 1/1, 2/1, and 5/1), more zigzag nanowires with a larger size occur, and a new one-dimensional nanostructure (i.e., nanoscrews) begins to appear for C/Ga molar ratios of 2:1 and 5:1. The zoomed-in SEM image of the nanoscrews in the inset of Figure 2f hints a 6-fold symmetric structure with a diameter of several tens to 100 nm modulated along their axes.

4. Plausible Growth Mechanism

When the amount of carbon is low in the starting mixture (i.e., C/Ga molar ratios of 1/10 and 1/5), most Ga_2O_3 would be directly nitridated to GaN:

$$Ga_2O_3 + 2NH_3 \rightarrow 2GaN + 3H_2O \quad (1)$$

Only a small amount of Ga_2O_3 would react with carbon to form gaseous Ga_2O, which then evaporates and reacts with NH_3 to form GaN as illustrated below:

$$Ga_2O_3 + 3C \rightarrow Ga_2O + 2CO \quad (2a)$$

$$Ga_2O + 2NH_3 \rightarrow 2GaN + H_2O + 2H_2 \quad (2b)$$

Consequently, porous structures would be formed as shown by the SEM images of Figure 2a,b. Due to the low C/Ga molar ratio in the starting mixture, MnO_2 would be mainly reduced to Mn_2O_3 and then to MnO, and only a small fraction of the Mn atoms in the starting mixture would be doped into the GaN lattice.

When the C/Ga molar ratio is increased in the starting mixture, more gaseous Ga_2O is generated and evaporated to the surface of the porous structures, then reacting with NH_3 to form zigzag GaN nanowires as shown in Figure 2c,d. When the C/Ga molar ratio is increased further, GaN nanoscrews appear with zigzag nanowires (Figure 2e,f) while the formation of a cubic MnO phase disappears and the amount of Mn atoms doped into GaN increases.

The HR-TEM micrographs and the selected-area electron diffraction (SAED) patterns of zigzag nanowires and nanoscrews are presented in Figure 3a,b. The diffraction patterns as well as the measured spacing along the growth directions confirm that the zigzag nanowires are growing along ⟨100⟩, whereas the nanoscrews are growing along ⟨001⟩. According to the growth mechanism of stacked cones and smooth nanowires of GaN reported by Cai et al.,[15] different growth directions are preferred under different conditions; namely, ⟨001⟩ is preferred under a N-rich condition and ⟨100⟩ under a Ga-rich condition. Stacked cones and smooth nanowires are synthesized by varying the flow rate of NH_3. In our experiments, the flow rate of NH_3 was kept constant during the synthetic process. Nevertheless, the switch from a N-rich to a Ga-rich condition should occur, because the amount of Ga_2O generated by the reaction between Ga_2O_3 and C will be different at different stages of the experiment. In the beginning of the experiment, Ga_2O_3 and activated charcoal are mixed uniformly in the starting mixture and hence can react with each other easily. The ratio of Ga_2O to NH_3 is relatively high on the surface of the porous structures. As the experiment goes on, both Ga_2O_3 and carbon are consumed, thereby reducing the amount of Ga_2O and lowering the ratio of Ga_2O to NH_3. As a result, a N-rich condition is found as the experiment proceeds.

To test the above suggestion, Mn-doped GaN was synthesized from the starting mixture with a C/Ga molar ratio of 5/1 by changing the nitridation time from 1 to 3 h. The resulting SEM images are shown in Figure 3c,e. For the shortest reaction time, a uniform morphology of zigzag nanowires is found (Figure 3c). When the reaction time is increased, a mixed morphology of zigzag nanowires and nanoscrews is observed (Figures 3d and 4b).

The formation of zigzag nanowires and nanoscrews could be explained using the imperfect oriented attachment (OA) mechanism, which is a promising route for the fabrication of complex-shaped nanostructures.[16−18] According to the OA

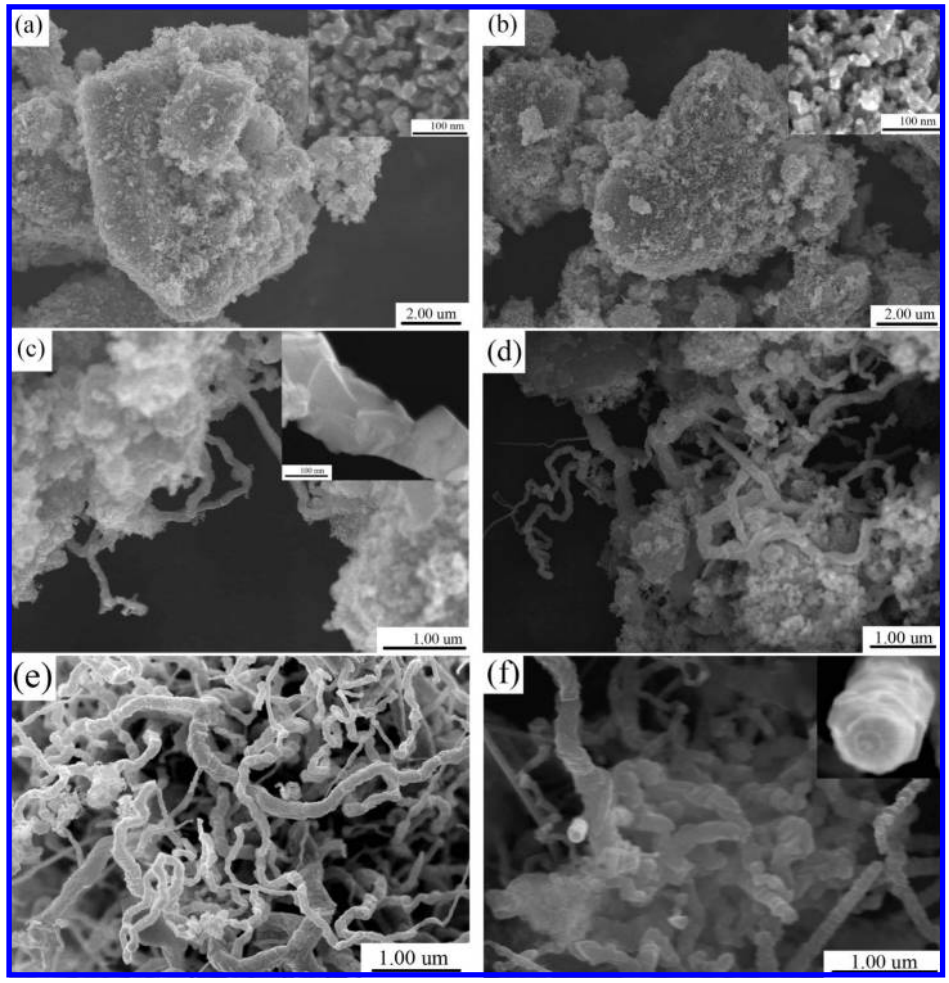

Figure 2. SEM images of the as-grown samples of Mn-doped GaN from the mixture of the starting materials with C/Ga molar ratios of (a) 1/10, (b) 1/5, (c) 1/2, (d) 1/1, (e) 2/1, and (f) 5/1.

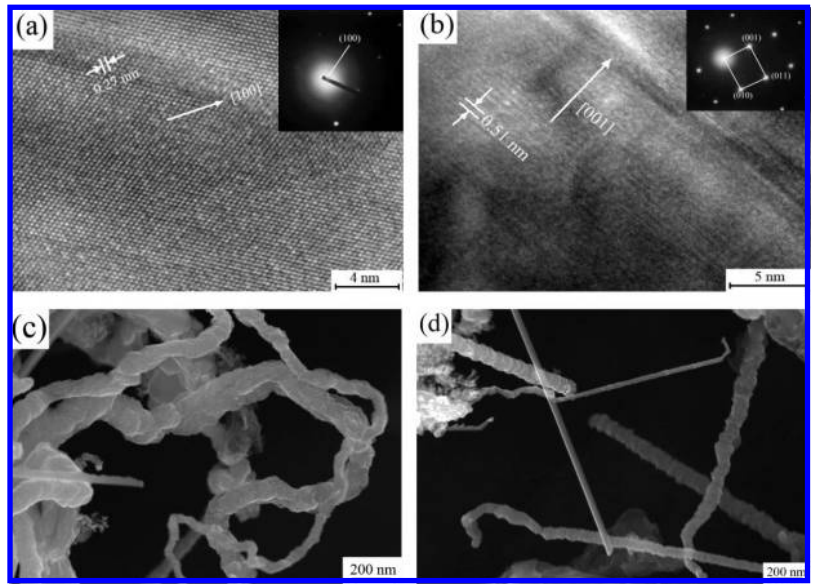

Figure 3. SAED patterns of the (a) zigzag nanowires and (b) nanoscrews found for the as-grown sample from the starting mixture with a C/Ga molar ratio of 5/1 and SEM images of the as-grown sample from the starting mixture with a C/Ga molar ratio of 5/1 by nitridation for (c) 1 h and (d) 3 h.

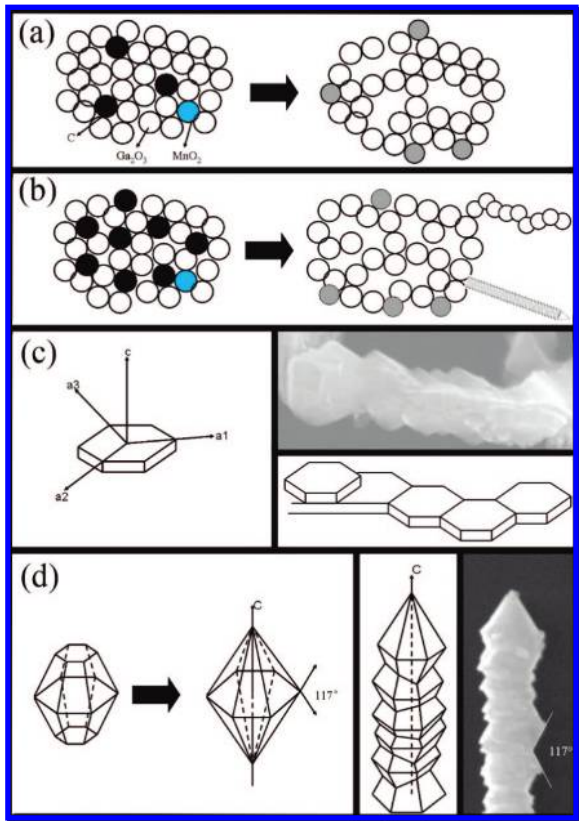

Figure 4. Schematic diagrams illustrating the growth mechanism: (a) porous structures from the starting mixture with a low C/Ga molar ratio, (b) zigzag nanowires and nanoscrews from the starting mixture with a high C/Ga molar ratio, (c) zigzag nanowires with hexagonal facet growth units attached to one of the three *a* axes, (d) nanoscrews formed by oriented attachment along the ⟨001⟩ direction. The angle between the two edges of the hexagonal cones is 117°, which is consistent with the value estimated from the SEM image.

process, the crystals grow along a crystallographically specific direction and only the facets with the same or similar surface energies and lattice orientations can attach together. Under a Ga-rich condition, the growth along the ⟨100⟩ direction is preferred, and hexagonal GaN facet growth units are formed and attached randomly along one of the three *a* axes of the unit cell, as illustrated in Figure 4c. Under a Ga-poor condition, the growth along ⟨001⟩ can be as likely as that along the ⟨100⟩ direction. The growth unit would be transformed from a hexagonal facet to a hexagonal cone with 12 {101} planes as the side surfaces. These growth units attach and grow along the *c* axes as illustrated in Figure 4d. The angle between two edges of {2−13} is 117°, which is consistent with the value estimated from the SEM images shown in Figure 4d.

5. XPS Measurements

To investigate the states of the C and Mn atoms incorporated into GaN, the binding energies of the C 1s and Mn $2p_{3/2}$ states were measured for the as-grown samples by XPS (Figure 5). The XPS spectra were charge corrected to the adventitious C 1s peak at 284.8 eV. The C 1s peaks of all as-grown samples can be deconvoluted into five components at 283.6, 284.8, 285.9, 287.4, and 290.3 eV. The peak at 283.6 eV, a lower binding energy compared with that of the C 1s peak for the adventitious carbon (284.8 eV), indicates the presence of C−Ga bonds (i.e., C at a N site). The peak at 285.9 eV can be attributed to the nitrile-like bonds (−C≡N),[19] which are produced during the nitridation process and adsorbed to the GaN surface. The peaks at 287.4 and 290.3 eV are due to adsorbed carbon species (e.g., C−O and C═O bonds). As the C/Ga ratio increases in the starting mixture, the peak at 284.8 eV arising from the residual C of the starting material increases constantly, and the peak at 283.5 eV also increases slightly. The latter indicates the formation of more C−Ga bonds and hence the incorporation of more C atoms into the N sites rather than into the Ga sites

(15) Cai, X. M.; Djurišić, A. B.; Xie, M. H.; Chiu, C. S.; Gwo, S. *Appl. Phys. Lett.* **2005**, *87*, 183103.
(16) Banfield, J. F.; Welch, S. A.; Zhang, H.; Ebert, T. T.; Penn, R. L. *Science* **2000**, *289*, 751.
(17) Penn, R. L.; Banfield, J. F. *Science* **1998**, *281*, 969.
(18) Adachi, M.; Murata, Y.; Takao, J.; Jiu, J.; Sakamoto, M.; Wang, F. *J. Am. Chem. Soc.* **2004**, *126*, 14943.
(19) Kucheyev, S. O.; Bradby, J. E.; Li, C. P.; Ruffell, S.; van Buuren, T.; Felter, T. E. *Appl. Phys. Lett.* **2007**, *91*, 261905.

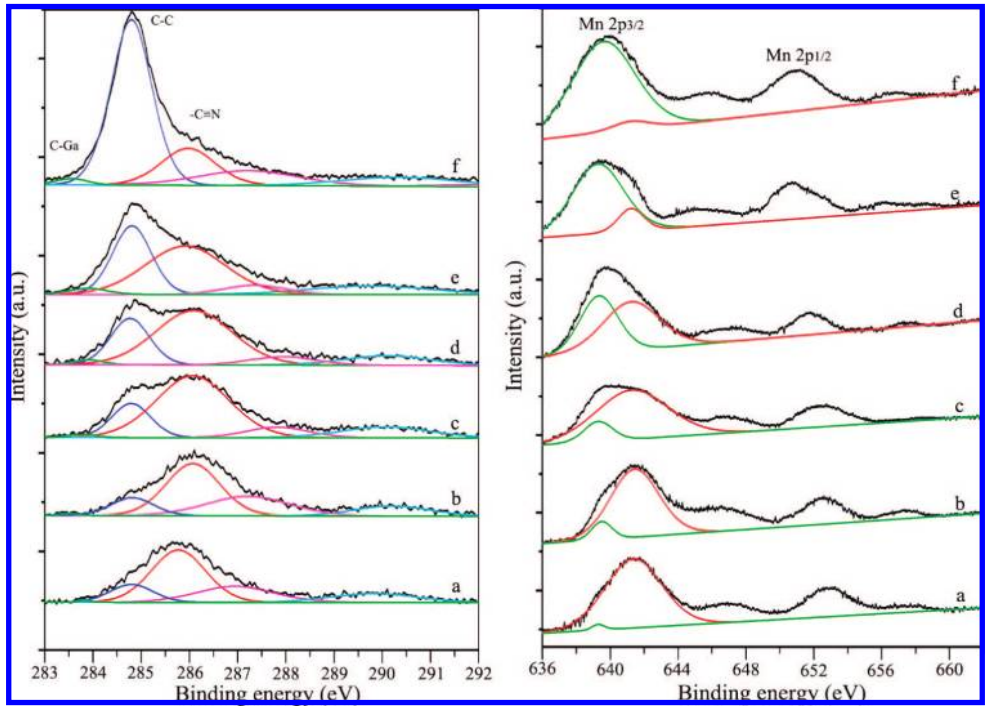

Figure 5. XPS spectra of the (a) C 1s and (b) Mn 2p states of the as-grown samples from starting mixtures with different C/Ga ratios. The labels a, b, c, d, e, and f indicate the as-prepared samples from the mixture of starting materials with C/Ga molar ratios of 1/10, 1/5, 1/2, 1/1, 2/1, and 5/1, respectively.

Table 1. Comparison of the Actual C/Ga, Mn/Ga, and C/Mn Ratios of the As-Grown Mn/C-Doped GaN Samples Determined from the C 1s, Mn 2p, and Ga 3d XPS Measurements

sample	nominal C/Ga	actual C/Ga	actual Mn/Ga	actual C/Mn
a	1/10	0.0017	0.0019	0.89
b	1/5	0.0016	0.0020	0.80
c	1/2	0.0054	0.0062	0.87
d	1/1	0.0089	0.0117	0.76
e	2/1	0.0155	0.0180	0.86
f	5/1	0.0234	0.0271	0.86

when the C/Ga ratio increases in the starting mixture. Namely, a C atom doping into the GaN lattice favors a N site over a Ga site. This conclusion was confirmed by performing first-principles DFT electronic structure calculations on model C-doped structures of GaN (see section 7).

The actual C/Ga ratio in each as-grown sample was determined by comparing the integrated peak area of the deconvoluted C 1s peak corresponding to the carbide with that of the Ga 3d XPS peak. As summarized in Table 1, the actual C/Ga ratio in any as-grown sample is considerably smaller than the nominal C/Ga ratio in the starting mixture by a factor of ~110 on average. Nevertheless, the actual C/Ga ratio in the as-grown sample increases gradually with increasing nominal C/Ga ratio in the starting mixture.

The Mn 2p XPS spectra of the as-grown samples are presented in Figure 4c. The Mn $2p_{3/2}$ and Mn $2p_{1/2}$ peaks are centered around ~641 and 652 eV with satellite peaks at higher binding energies (646.5 and 657.5 eV, respectively), which shows that the Mn atoms in the as-grown samples are in the divalent state,[20] a feature not present in either Mn_2O_3 (Mn^{3+}, 641.7 eV) or MnO_2 (Mn^{4+}, 642.5 eV). The Mn $2p_{3/2}$ peak can be deconvoluted into two peaks at 639.8 and 641.2 eV. The peak at 641.2 eV can be attributed to a Mn−O bond according to the reported binding energy of MnO (Mn^{2+}, 641 eV).[21] The peak at 639.8 eV, a lower binding energy for a Mn−O bond, can be due to the formation of a Mn−N bond. The Mn−O peak is predominant when the C/Ga ratio (either nominal or actual) is low. As the C/Ga ratio increases, the Mn−O peak decreases while the Mn−N peak increases. This is in agreement with the observation from the XRD measurements that the MnO phase gradually disappears as the C/Ga ratio increases. The Mn−N subpeak should arise from the Mn atoms incorporated into the GaN lattice, because no Mn/N binary phase is detected in the XRD spectra. Thus, it is concluded that Mn atoms are incorporated into the GaN lattice by occupying the Ga sites, and the extent of this incorporation increases with increasing C/Ga ratio in the starting mixture.

The actual atom ratio, Mn/Ga, of each as-grown sample determined from the areas of the Mn−N subpeak and Ga 3d XPS peak is listed in Table 1. As can be seen, the actual Mn/Ga ratio of the as-grown sample increases steadily with increasing C/Ga ratio of the starting mixture and is smaller than the corresponding value in the starting mixture (i.e., 5%). The sample with the highest C/Ga ratio has a Mn/Ga value of 2.7%, which is more than 10 times greater than that found for the sample with the lowest C/Ga ratio.

The presence of the XPS peaks associated with Mn−N and C−Ga environments shows that both Mn and C atoms are successfully doped into the GaN lattice during the nitridation process. The actual C/Mn atom ratios of the as-grown samples estimated from the actual C/Ga and Mn/Ga atom ratios are listed in Table 1. The actual C/Mn ratios are nearly independent of the nominal C/Ga ratio in the starting mixture and are close to 0.84 on average. That is, the extent of C incorporation is comparable to that of Mn incorporation

(20) Jeng, S. P.; Lad, R. J.; Henrich, V. E. *Phys. Rev. B* **1991**, *43*, 11971.

(21) Audi, A. A.; Sherwood, M. A. *Surf. Interface Anal.* **2002**, *33*, 274.

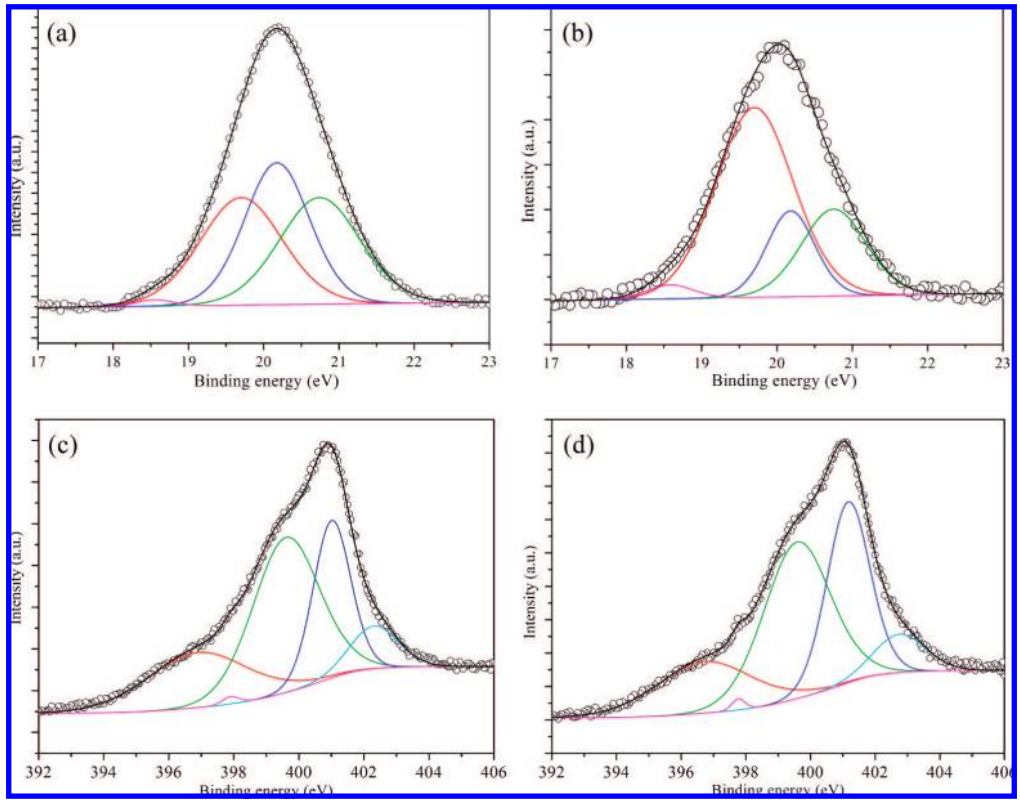

Figure 6. Deconvolution of the Ga 3d XPS peaks for the as-grown sample from the starting mixture with C/Ga ratios of (a) 1/1 and (b) 5/1 and deconvolution of the N 1s XPS peaks for the as-grown sample from the starting mixture with C/Ga ratios of (c) 1/1 and (d) 5/1.

in the GaN matrix, and this suggests that Mn/C-codoping is energetically favorable.

The Ga 3d and N 1s XPS spectra of the as-prepared samples from the starting mixture with C/Ga ratios of 1/1 and 5/1 are presented in Figure 6, where the empty circles represent the original data and the solid lines the fitted curves in terms of the deconvoluted individual peaks. The Ga 3d spectra are deconvoluted into four peaks at 18.5, 19.7, 20.2, and 20.8 eV. The peaks at 19.7 and 20.8 eV are assigned to the Ga−N and Ga−O bonds, respectively. The other peaks at 18.5 and 20.2 eV are attributed to the Ga−C and Ga−N/O bonds that originate from the intermediate phases such as amorphous GaN and GaON.[22,23] For the as-prepared sample from the starting mixture with a C/Ga ratio of 1/1, the peak areas of the Ga 3d XPS spectrum are 32.8% for the Ga−N bond, 31.95% for the Ga−O bond, 0.89% for the Ga−C bond, and 34.35% for the Ga−N/O bond. When the C/Ga ratio is increased to 5/1 in the starting mixture (Figure 6b), the peak area of the Ga−N bond increases to 58.61%, that of the Ga−O bond decreases to 22.4%, and that of the Ga−C bond increases to 2.56%. These changes are significant and show that the presence of C in the starting mixture helps reduce the oxide content in the as-prepared samples and the higher C content in the starting mixture helps introduce more C atoms into the as-prepared samples. The latter is consistent with our XRD results discussed in the previous section.

The N 1s peak consists of five components at 396.7, 397.8, 399.6, 401.2, and 402.7 eV (Figure 6c,d). The peaks at 396.7 and 397.8 eV can be attributed to N−Ga and N−Mn bonds, respectively. The peak at 399.6 eV is the value expected for free amine, and that at 401.2 and 402.7 eV can be attributed to N≡C and N−O bonds, respectively. For the sample obtained from the starting material with a C/Ga ratio of 1/1, the ratio of the peak area of the N−Mn bond to that of the N−Ga bond is about 0.032. For the sample with a C/Ga ratio of 5/1 in the starting material, the corresponding ratio is 0.045. Thus, from the Ga 3d peak and the N 1s peaks, the Mn/Ga ratios are calculated to be be 0.011 and 0.026 for the samples obtained from the starting material with C/Ga ratios of 1/1 and 5/1, respectively. These results are in good agreement with the Mn/Ga ratios calculated from the C 1s and Mn 2p peaks.

6. Magnetic Properties

The magnetic properties of the as-grown samples were studied by measuring their magnetization, **M**, as a function of the magnetic field, **H**, at room temperature (Figure 7a). All the samples show a weak but discernible hysteresis indicative of ferromagnetic interactions in the samples. The saturation magnetization, $\mathbf{M}_s$, depends greatly on the C/Ga molar ratio of the starting mixture, and the highest $\mathbf{M}_s$ of 0.122 emu/g results from the as-grown sample with the highest C/Ga molar ratio of 5/1. The latter is greater than the corresponding value found for the Mn-doped GaN without C-codoping (i.e., 0.0028 emu/g) by a factor of ∼40. The actual Mn/Ga ratio and the $\mathbf{M}_s$ value of Mn/C-codoped GaN increase steadily with increasing C/Ga molar ratio (Figure 7b). This reflects that when the C/Ga molar ratio is increased, the extent of Mn-doping into the GaN lattice increases steadily, thereby enhancing the ferromagnetism of the as-grown sample. Our results are in support of Wang et al.'s

(22) Wolter, S. D.; Delucca, J. M.; Mohney, S. E.; Kern, R. S.; Kuo, C. P. *Thin Solid Films* **2004**, *371*, 153.
(23) Kuball, M.; Mokhtari, H.; Cherns, D.; Lul, J.; Westwood, D. I. *Jpn. J. Appl. Phys.* **2000**, *39*, 4753.

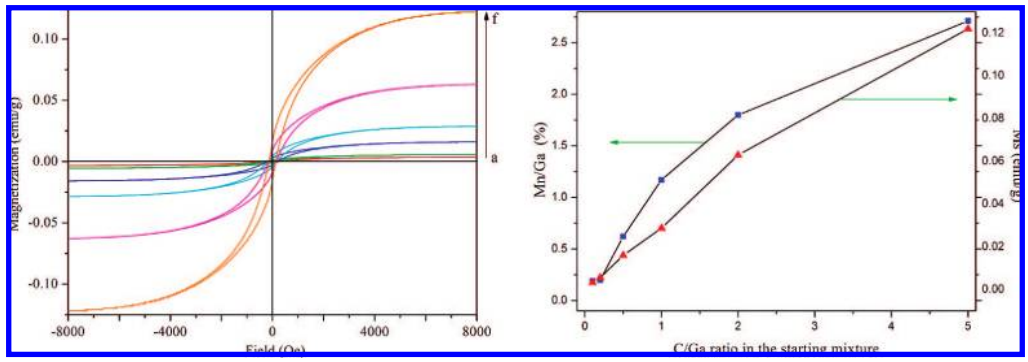

Figure 7. (a) Magnetization vs magnetic field measured at room temperature for the as-grown Mn/C-doped GaN samples from the starting mixture with C/Ga ratios of 1/10, 1/5, 1/2, 1/1, 2/1, and 5/1. The $\mathbf{M}_s$ values increase gradually with increasing C/Ga ratio, with the highest saturation magnetization $\mathbf{M}_s$ of 0.122 emu/g found for a C/Ga molar ratio of 5/1. (b) Values of the actual Mn/Ga ratio (atom %) and $\mathbf{M}_s$ (μ_B) of the as-grown Mn/C-doped GaN samples as a function of the nominal C/Ga ratio in the starting mixture.

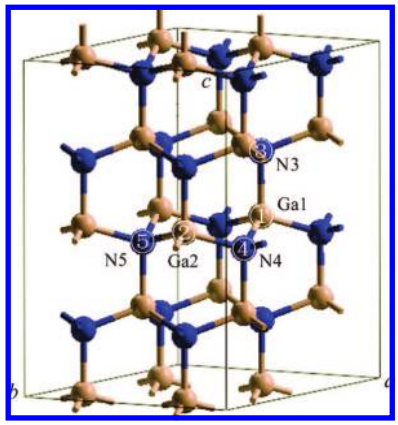

Figure 8. Supercell (32-atom, 2 × 2 × 2) of GaN used for the simulation of Mn/C-doping, where the gray and blue spheres represent Ga and N atoms, respectively. The five doping sites employed in our calculations are numbered 1−5.

theoretical prediction[24] that the ferromagnetism of Mn-doped GaN is enhanced by codoping with carbon.

7. Energetics of Mn/C-Doping in the GaN Matrix

To examine the site preference of C-doping and the possible cooperative effect of Mn/C-codoping in the GaN matrix, we carried out first-principles spin-polarized DFT electronic structure calculations using the Vienna Ab-Initio Simulation Package[25,26] for eight model doped structures constructed on the basis of a 32-atom 2 × 2 × 2 supercell. As depicted in Figure 8, the five doping sites used for our calculations are numbered 1−5.

The eight model doped structures examined in our study are (1) $Ga_{15}N_{16}C$ with C at Ga1, (2) $Ga_{16}N_{15}C$ with C at N3, (3) $Ga_{15}MnN_{16}$ with Mn at Ga1, (4) $Ga_{14}Mn_2N_{16}$ with Mn at Ga1 and Ga2 so that the two Mn atoms are at the nearest-neighbor sites, (5) $Ga_{14}Mn_2N_{15}C$ with two Mn atoms at Ga1 and Ga2 and one C at N3, (6) $Ga_{15}MnN_{15}C$ with Mn at Ga1 and C at N3 so that the Mn and C atoms are at the next-nearest-neighbor sites, (7) $Ga_{15}Mn\ N_{15}C$ with Mn at Ga1 and C at N4 so that the Mn and C atoms are at the nearest-neighbor sites, and (8) $Ga_{15}MnN_{15}C$ with Mn at Ga1 and C at N5 so that the Mn and C atoms are at far distant sites.

Table 2. Total Energies (eV) and Total Moments (μ_B) Calculated for the Eight Doped Models Constructed Using a 32-Atom 2 × 2 × 2 Supercell of GaN

	doping site	total energy[a]	total moment/ supercell
$Ga_{15}N_{16}C$	C@Ga1	−201.682	0.45
$Ga_{16}N_{15}C$	C@N2	−198.675	0.14
$Ga_{15}MnN_{16}$	Mn@Ga1	−205.577	4.00
$Ga_{14}Mn_2N_{16}$	Mn@Ga1,Ga2	−210.154 (FM)	8.06
		−210.138 (AFM)	0.00
$Ga_{14}Mn_2C\ N_{15}$	Mn@Ga1,Ga2, C@N_4	−209.345 (FM)	7.00
		−208.989 (AFM)[a]	1.33
$Ga_{15}MnN_{15}C$	Mn@Ga1, C@N3	−204.402 (FM)	3.01
		−204.402 (AFM) [a]	3.02
$Ga_{15}Mn\ N_{15}C$	Mn@Ga1, C@N4	−204.020 (FM)	1.00
		−203.866 (AFM)[a]	0.93
$Ga_{15}MnN_{15}C$	Mn@Ga1, C@N5	−203.600 (FM)	3.00
		−203.601 (AFM)[a]	3.00

[a] FM and AFM indicate that the moments of the Mn and C sites are ferromagnetically and antiferromagnetically oriented, respectively.

Our calculations employed the generalized gradient approximation (GGA),[27] the exchange-correlation functional of Perdew, Burke, and Ernzerhof,[28] a plane wave cutoff energy of 400 eV for the basis set, and the sampling of the irreducible Brillouin zone with 4 × 4 × 4 Monkhorst−Pack k points for the supercell.[29] In our calculations, the cell parameters were fixed at the experimental values (i.e., $a = b = 3.189$ Å and $c = 5.185$ Å for undoped GaN), and all atomic positions were optimized until all forces became smaller than 10^{-4} eV/Å. The results of our calculations are summarized in Table 2.

To examine the site preference of a C-doping in the GaN lattice, it is necessary to compare the substitution energies for the following processes at the standard state:

$$[GaN] + C \rightarrow [GaN \text{ with } C@Ga] + [Ga] \text{ (solid at 298 K)} \ (\Delta H_{Ga})$$

$$[GaN] + C \rightarrow [GaN \text{ with } C@N] + (1/2)N_2 \text{ (gas at 298 K)} \ (\Delta H_{N})$$

Therefore, the energy difference between ΔH_{Ga} and ΔH_N can be obtained by comparing the sum of the total energies on the right-hand side. Our VASP calculations show that the energy of elemental Ga (solid at 298 K) is −2.178 eV per Ga and that of N_2 (gas at 298 K with N−N = 1.11 Å) is −16.518 eV per

(24) Wang, Q.; Sun, Q.; Jena, P. *Phys. Rev. B* **2007**, *75*, 35322.
(25) Kresse, G.; Furthmüller, J. *Comput. Mater. Sci.* **1996**, *6*, 15.
(26) Kresse, G.; Furthmüller, J. *Phys. Rev. B* **1996**, *54*, 11169.
(27) Perdew, J. P.; Wang, Y. *Phys. Rev. B* **1992**, *45*, 13244.
(28) Perdew, J. P.; Burke, K.; Ernzerhof, M. *Phys. Rev. Lett.* **1996**, *77*, 3865.
(29) Monkhorst, H. J.; Pack, J. D. *Phys. Rev. B* **1976**, *13*, 5188.

formula unit. Thus, given the calculated total energies of $Ga_{15}N_{16}C$ and $Ga_{16}N_{15}C$ listed in Table 2, it is estimated that ΔH_N is lower in energy than ΔH_{Ga} by about 2.5 eV per 16 formula units of GaN. Namely, a C atom doping in GaN favors a N site over a Ga site. This is consistent with our conclusion from the analysis of the C 1s XPS peaks of Mn/C-doped GaN (see section 5).

Table 2 shows that doping of one Mn at a Ga site generates 4 μ_B and that of one C at a N site generates a very small moment (0.14 μ_B). For the cases of one Mn@Ga and one C@N, the total moment is close to 3 μ_B when the energy difference between the FM and AFM states is negligible (namely, Mn@Ga1 with C@N3 and Mn@Ga1 with C@N5), but is substantially reduced (i.e., $\sim$1 μ_B) when the FM state is favored over the AFM state (i.e., Mn@Ga1 with C@N4). The fact that the Mn/C-codoping leads to a smaller total moment than does Mn-only doping is consistent with the report of Wang et al.[24] The comparison of the case of two Mn@Ga's (i.e., Mn atoms at the Ga1 and Ga2 sites) with that of two Mn@Ga's and one C@N (i.e., Mn atoms at the Ga1 and Ga2 sites and a C atom at the N4 site) shows that the C-codoping strongly enhances the preference of the FM coupling over the AFM coupling between the two doped Mn sites. This finding is in support of the theoretical prediction by Wang et al.[24]

Our calculations show that the formation energy $\Delta H_{Mn/C}$ for one Mn and one C in GaN ($\Delta H_{Mn/C} = E$[GaN with Mn and C] $- E$[GaN with C] $+ E$[Ga]) is lower than the formation energy ΔH_{Mn} for one Mn in GaN ($\Delta H_{Mn} = E$[GaN with Mn] $- E$[GaN] $+ E$[Ga]) by about 1.8 eV per 16 formula units of GaN. This indicates that Mn-doping into the GaN lattice is enhanced by codoping with C. Therefore, it is expected that a higher Mn concentration in GaN can be achieved by codoping with C, thereby greatly enhancing the ferromagnetism. This is consistent with our experimental results.

Experimentally, the ferromagnetism in Mn/C-codoped GaN samples is observed for Mn/C-codoped GaN nanostructures, while the present calculations were carried out for the bulk structure.[30] In their recent first-principles DFT study of Cu-doped GaN nanowires, Xiang and Wei showed that two Cu dopants are most stable when they are near each other and that, compared with those of bulk GaN:Cu, magnetization and ferromagnetism in Cu-doped GaN nanowires are strongly enhanced because the width of the Cu d band is reduced due to the one-dimensional nature of the nanowires. To fully analyze the origin of the ferromagnetism in Mn/C-codoped GaN samples, use of a realistic model doped structure (e.g., nanostructures rather than bulk structures) is necessary. Such a study is beyond the scope of the present experimental work.

(30) Xiang, H. J.; Wei, S.-H. *Nano Lett.* **2008**, *8*, 1825.

8. Concluding Remarks

In summary, we have synthesized Mn/C-codoped GaN by carbothermal nitridation using activated charcoal as the carbon source. The bonding states of Mn and C atoms, characterized by XPS, confirm the doping of both Mn and C atoms into the GaN lattice. Nanostructures such as zigzag nanowires, nanoscrews, and hexagonal nanocones can be produced by controlling the reaction time and the C/Ga molar ratio in the starting mixture. Room-temperature magnetization measurements show that the saturation magnetization of Mn/C-codoped GaN can be greater than that of Mn-doped GaN by a factor up to $\sim$40 and increases steadily with increasing Ga/C molar ratio in the starting mixture at a rate of $\sim$0.023 emu/g per C/Ga molar ratio. Further investigations are necessary to learn how to control the morphology and the ferromagnetism of Mn-doped GaN more precisely. Our DFT calculations support the experimentally deduced suggestion that carbon doping in GaN favors the N sites over the Ga sites, Mn/C-codoping in the GaN matrix is energetically favorable, and the C-codoping strongly enhances the preference of the FM coupling over the AFM coupling between the two doped Mn sites. Further investigations are necessary to learn how to control the morphology and the ferromagnetism of Mn-doped GaN more precisely.

Acknowledgment. This work was financially supported by research grants from the National Basic Research Program of China (No. 2007CB613302) and the National Natural Science Foundation of China (Nos. 50721002, 10774091, and 50672052). M.-H.W. is thankful for the support by the Office of Basic Energy Sciences, Division of Materials Sciences, U.S. Department of Energy, under Grant DE-FG02-86ER45259.

JA807030V